

Mechanical Oscillations at the Cellular Scale

Frank Jülicher

Institut Curie, Physicochimie Curie, Section de Recherche, 26 rue d'Ulm, 75248 Paris
Cedex 05, France

Abstract. Active phenomena which involve force generation and motion play a key role in a number of phenomena in living cells such as cell motility, muscle contraction and the active transport of material and organelles. Here we discuss mechanical oscillations generated by active systems in cells. Examples are oscillatory regimes in muscles, the periodic beating of axonemal cilia and flagella and spontaneous oscillations of auditory hair cells which play a role in active amplification of weak sounds in hearing. As a prototype system for oscillation generation by proteins, we discuss a general mechanism by which many coupled active elements such as motor molecules can generate oscillations.

Keywords: biophysics/motility/oscillations/hearing/axoneme

Abstract. Les phénomènes actifs impliquant la génération de forces et de mouvement, jouent un rôle primordial dans de nombreux phénomènes de la vie cellulaire tels que la motilité, la contraction musculaire et le transport actif d'organelles ou de composés. Nous discutons ici les oscillations mécaniques générées par des systèmes actifs dans les cellules. Des exemples sont les régimes oscillatoires des muscles, le battement périodique des cils et des flagelles axonémaux et les oscillations spontanées des cellules auditives. Ces oscillations spontanées ci pourraient jouer un rôle important dans l'audition par l'amplification des faibles sons. Nous discutons un système prototype de génération d'oscillations par des protéines, en décrivant un mécanisme général impliquant l'intervention de nombreux éléments actifs, comme des moteurs moléculaires.

Mots clés: biophysique/motilité/oscillations/audition/axoneme

1 Introduction

The generation of forces and the ability to move represent some of the most striking abilities of living cells. Prominent examples are cell motility, the contraction of muscles but also active transport of materials and of organelles, for example during cell division and mitosis. Such movements are generated on the molecular level by protein molecules that convert chemical energy to mechanical work. Prominent examples are linear motor proteins of eucariotic cells. These motors are specialized to work by interacting with filaments of the cytoskeleton [1]. They consume Adenosintriphosphate (ATP) as a fuel and convert its chemical energy to mechanical work. Myosin motors for example generate motion along actin filaments. They are the active components in muscles, while kinesin and dynein motors move along microtubules [2].

In certain situations, cells can generate oscillatory motion and operate as mechanical oscillators. Oscillatory behaviors of muscles have been known for a long time in the case of some flight muscles which move the wings of insects [3]. Many insects such as wasps and bees have muscles called "asynchronous" which generate oscillatory contractions by a mechanism located in the muscle itself which drives the beating of the wings. This type of muscle differs from "synchronous" flight muscles of some other insects for which contractions are triggered by a periodic nerve signal and are not generated in the muscle. More recently, oscillatory behaviors have been observed under certain conditions in fibrils of ordinary skeletal muscles which under normal conditions do not oscillate [4, 5].

An important example for mechanical oscillations on the cellular scale is the periodic motion of cilia and flagella [6, 7]. These hair-like appendages of many cells are used for swimming and self-propulsion by sperm and some small organisms or to stir fluids surrounding a cell or cell layer. The common structural feature of these cilia and flagella is the axoneme, a well conserved arrangement of microtubule doublets organized in a cylindrical fashion. Dynein molecular motors are attached to these microtubules and can exert forces on neighboring microtubules. This structure is very well conserved and appears in a large number of different cells of different organisms [8]. The activity of the dynein molecular motors coupled to the microtubules leads to periodic bending deformations and waves along the cilium. In the case of sperm, the flagellum propagates bending waves from the head towards the tail [9]. These waves are very regular and essentially planar [10, 11] and break the necessary symmetries to allow the sperm to swim in a viscous solution [12, 13].

In the following sections, we describe some properties of mechanical oscillators and their implications for biological situations. Close to an oscillating instability called Hopf-bifurcation [14], the behavior of a mechanical oscillator and its response to externally imposed oscillating forces are generic [15, 16]. As a prototype system for the generation of oscillations in cells, we discuss a general mechanism by which a large number of active elements such as molecular motors which are coupled to an elastic element and which undergo a chemical cycle of fuel consumption can generate mechanical oscillations [17, 18]. These oscillations are a result of collective behavior of many motors [19, 20] which can give rise to different types of dynamic transitions [17, 21, 22, 23]. The same physical mechanism can also generate oscillatory modes and bending waves along elastic filaments which interact with many motors as in the case of cilia [24, 25, 26]. Finally, oscillating instabilities can play an important role in sensory systems. A lot of evidence points to an active system involved in the detection of sound by the ear [27, 29, 30, 31]. The inner ear shows a frequency selective nonlinear response to sound stimuli and actively amplifies weak sounds [32]. These properties allow the ear to cover a large dynamic range of 120dB and to detect weak sounds which per cycle of oscillation impart an energy that is less than kT [33]. These properties of the ear can be understood if we assume that the inner ear contains dynamical systems which operate at Hopf bifurcation with critical fre-

quencies that cover the audible range. A simple self-tuning mechanism involving a feedback control can explain how these systems tune reliably to their critical point. The concept of a self-tuned Hopf bifurcation can explain many apparently distinct phenomena observed in hearing such as otoacoustic emissions, nonlinearities, adaptation and fatigue as well as the response to complex sounds in a unified framework [15, 34].

2 Mechanical oscillators

A large variety of nonlinear dynamic systems is capable to generate periodic, oscillating motion. In order to illustrate some of the general properties of mechanical oscillators, we consider a dynamical system related to the Van der Pol oscillator which is standard model for nonlinear oscillators [35, 36]. Consider the dynamic equations

$$\gamma\ddot{x} + r\dot{x} - \Lambda\dot{x}^3 + kx = f_{\text{ext}}(t) \quad , \quad (1)$$

which represent a damped oscillator with additional nonlinear friction. Here x is a displacement variable and f_{ext} an external force. We assume that γ , k and Λ are positive parameters and that r can become negative. Note that while the term characterized by γ could be an inertial term, we will consider in the following only situations where all inertial terms are neglected. However, γ is in this case nonzero and arises from the intrinsic dynamics of the system.

In the absence of external forces, the system is stable for $r > 0$. It shows damped oscillations or is overdamped, and relaxes to $x = 0$. For $r = 0$, the system becomes unstable and undergoes a Hopf-bifurcation. For $r < 0$ spontaneous oscillations are generated. In this regime the nonlinearity characterized by Λ is essential to stabilize the system and to determine the oscillation amplitude. In the periodic limit cycle for $f_{\text{ext}} = 0$, we can write

$$x(t) = \sum_n x_n e^{in\omega t} \quad (2)$$

as a Fourier sum with oscillation frequency ω . Close to the bifurcation point, i.e. for small but negative r , the first Fourier mode x_1 dominates and obeys to lowest order

$$\mathcal{A}x_1 + \mathcal{B}|x_1|^2x_1 = 0 \quad (3)$$

Here, higher modes $x_n \sim x_1^n$ are neglected and the complex coefficients are given by $\mathcal{A} = k - \gamma\omega^2 + i\omega r$ and $\mathcal{B} = 3i\Lambda\omega^3$. Spontaneous oscillations occur with frequency $\omega = \omega_c \equiv (k/\gamma)^{1/2}$. This is the only choice for which Eq. (3) has a solution for which the oscillation amplitude

$$|x_1|^2 = -\frac{\mathcal{A}}{\mathcal{B}} = -\frac{r\gamma}{3\Lambda k} \quad (4)$$

is real and positive. The bifurcation point $r = 0$ is characterized by the condition that $\mathcal{A} = 0$ vanishes at the critical frequency $\omega = \omega_c$. If this system is subject

to an external force $f_{\text{ext}} = 2f_1 \cos(\omega_{\text{ext}}t)$ with frequency ω_{ext} , there are two frequencies in the system, the spontaneous frequency and the externally imposed one. For simplicity, we focus on the situation where only one frequency is present, i.e. the system is either outside the spontaneously oscillating regime ($r \geq 0$), or both frequencies are the same $\omega = \omega_{\text{ext}}$. In this case, Eq. (3) becomes simply

$$\mathcal{A}x_1 + \mathcal{B}|x_1|^2x_1 = f_1 \quad (5)$$

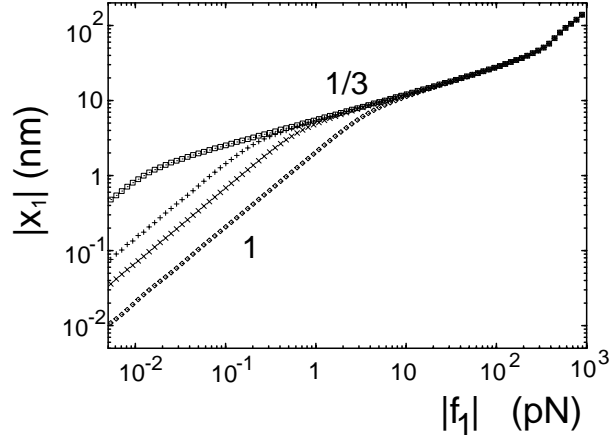


Fig. 1. Fourier amplitude $|x_1|$ of the response of a dynamical system at a Hopf bifurcation to a stimulus force of amplitude $|f_1|$ at different frequencies. The data is obtained by a numerical solution of the model described in the subsequent section, see [15]. The power law of the response is indicated.

This Equation is generic in the sense that all other terms can be neglected if the system is sufficiently close to its bifurcation point. We therefore focus on the case where $r = 0$ and the system is exactly at the bifurcation. Two different regimes of the response to an oscillating force can be distinguished, see Fig.1. If the applied frequency is close to the critical frequency, the linear term can be ignored and

$$|x_1| \simeq |\mathcal{B}|^{-1/3}|f_1|^{1/3} \simeq \frac{|f_1|^{1/3}}{3^{1/3}\mathcal{A}^{1/3}\omega_c} \quad (6)$$

If the frequency mismatch is larger, $|\omega - \omega_c| \gg |f_1^{2/3}| |\mathcal{B}|^{1/3}\gamma|\omega + \omega_c|$, the cubic term is unimportant and the response is linear

$$|x_1| \simeq |\mathcal{A}|^{-1}|f_1| = \frac{|f_1|}{\gamma|\omega^2 - \omega_c^2|} \quad (7)$$

The response of the system given by Eq. (5) together with the oscillation amplitude (4) characterize the main properties of an oscillator near the bifurcation

point. This approach can be generalized to situations where more than one frequency are present [34].

3 Oscillations generated by molecular motors

How can a system of the type described in the last section be realized using biological materials? A spontaneously oscillating system must be active, i.e. it has to consume energy from some input. Furthermore the system must be able to generate motion and active displacements. A prototype system for motion generation in cells are molecular motors which are enzymes that are driven by a chemical reaction (usually the hydrolysis of ATP) and which are able to generate motion and mechanical work. An individual motor behaves stochastically and generates on average motion in a preferred direction along a polar track filament. Because of the stochastic function of individual molecules, phase coherent oscillations can only be generated if many motors are involved and their fluctuations become unimportant for the collective behavior of the entire system.

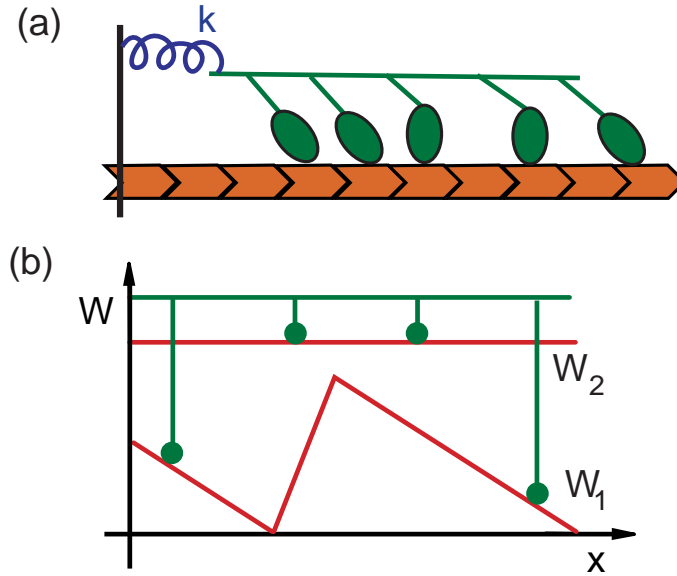


Fig. 2. (a) Schematic representation of many motors collectively working against a spring of elastic modulus k . (b) Two state model for many motors. Each state is characterized by an energy landscape $W_i(x)$.

We consider here a specific situation where a large number of molecular motors which are rigidly connected and coupled to elastic elements can undergo a Hopf-bifurcation [17], see Fig. 2 (a). This description is based on simple models

for the force generation of molecular motors [37, 38, 39, 41, 17, 42] generalized to situations where many motors are coupled [19, 20]. In the limit of a very large number of motors N , fluctuations in the motor function become irrelevant and the system can be described by simple mean-field equations [43]. We consider motors moving along a periodic linear structure of period ℓ , see Fig. 2 (b). In the context of a two-state model for the motors, we study the probability density $P(\xi, t)$ to find a motor at position ξ in state $i = 1, 2$, which is normalized, $P_1 + P_2 = \ell^{-1}$, and satisfies

$$\begin{aligned}\partial_t P_1 &= -v\partial_\xi P_1 - \omega_1 P_1 + \omega_2 P_2 \\ \partial_t P_2 &= -v\partial_\xi P_2 + \omega_1 P_1 - \omega_2 P_2\end{aligned}\quad (8)$$

Here, ω_1 and ω_2 are the rates of chemical transition between the two conformations of the motors. The velocity $v = \lambda^{-1}(f_{\text{ext}} + f_{\text{mot}} - kx)$ is generated by the sum of the externally applied force per motor f_{ext} , the average force

$$f_{\text{mot}} = - \int_0^\ell d\xi (P_1 \partial_\xi W_1 + P_2 \partial_\xi W_2) \quad (9)$$

generated per motor and an elastic force in presence of an elastic element of modulus k per motor. The total friction coefficient per motor is denoted λ . The energy landscapes W_i characterize the interaction with the filament and are usually considered to be periodic with period ℓ . Using the condition $\dot{x} = v$, the system can undergo a Hopf-bifurcation in the vicinity of which Eq. (5) is satisfied with linear and nonlinear coefficients

$$\begin{aligned}\mathcal{A}(\omega, C) &= i\omega\lambda + k - i\omega \int_0^\ell d\xi \partial_\xi R \frac{\partial_\xi (W_1 - W_2)}{\alpha + i\omega} \\ \mathcal{B}(\omega, C) &= i\omega^3 (F_{1,1,-1} + F_{1,-1,1} + F_{-1,1,1})\end{aligned}\quad (10)$$

where

$$F_{klm} = \int_0^\ell d\xi \left(\partial_\xi \frac{1}{\alpha + ik\omega} \left(\partial_\xi \frac{\partial_\xi R}{\alpha + i\ell\omega} \right) \right) \frac{\partial_\xi (W_1 - W_2)}{\alpha + im\omega} \quad (11)$$

Here, $\alpha(\xi) \equiv \omega_1(\xi) + \omega_2(\xi)$, $R \equiv \omega_2/\ell\alpha$, and we have assumed for simplicity that the potentials and transitions are symmetric with respect to $\xi \rightarrow -\xi$. The coefficients \mathcal{A} and \mathcal{B} are functions of frequency and also depend on other model parameters such as the transition rates ω_1 and ω_2 . We introduce a control parameter C which summarizes changes in the transition rates which keep α constant and which will be varied in order to cross the bifurcation point. C could represent the concentration of any agent that influences chemical rates, in the case of motor molecules for example those of ATP or Ca^{++} .

In order to discuss these somewhat uninformative expressions, we consider the simpler case where α is a constant. In this case, we find

$$\begin{aligned}\mathcal{A} &= k - \gamma(\omega)\omega^2 + i\omega r(\omega) \\ \mathcal{B} &= -3iK_{\text{eff}}^{(\text{nl})} \frac{\omega^3}{(\alpha^2 + \omega^2)(\alpha + i\omega)}\end{aligned}\quad (12)$$

Eq. (12) corresponds to Eq. (1), however with coefficients that depend on both the frequency and the control parameter C

$$\begin{aligned}\gamma(\omega) &= \frac{K_{\text{eff}}^{(2)}}{\alpha^2 + \omega^2} \\ r(\omega) &= \lambda - \frac{K_{\text{eff}}^{(2)}\alpha}{\alpha^2 + \omega^2}\end{aligned}\quad (13)$$

The effective Hookian and nonlinear elasticities of the cross-bridges

$$K_{\text{eff}}^{(2)}(C) = \int_0^\ell d\xi R \partial_\xi^2 (W_1 - W_2) \quad (14)$$

$$K_{\text{eff}}^{(4)}(C) = \int_0^\ell d\xi R \partial_\xi^4 (W_1 - W_2) \quad (15)$$

which are functions of C and characterize the second and fourth derivative of the effective potential of a motor in the bound state. Note that the elasticity $K_{\text{eff}}^{(2)}$ together with the chemical transitions generates an effective "mass" $\gamma(\omega)$ and a negative contribution to friction.

If the control parameter C is varied, the system undergoes for a critical value C_c a Hopf-bifurcation. This happens as soon as $K_{\text{eff}}^{(2)}$ takes a value for which $\mathcal{A}(\omega_c, C_c) = 0$ vanishes for a critical value of the frequency ω_c . In order to characterize this point, note first that the imaginary part of \mathcal{A} vanishes if $r = 0$, or $\lambda = \alpha\gamma$. The critical frequency at the bifurcation satisfies $\omega_c = (k/\gamma(\omega_c))^{1/2}$ and is thus given by

$$\omega_c = \left(\frac{\alpha k}{\lambda}\right)^{1/2}. \quad (16)$$

The range of frequencies that can be obtained by this mechanism depends on the range of effective elasticities $K_{\text{eff}}^{(2)}$ which can result from motor-filament interactions. If the motor is detached most of the time this elasticity is small $K_{\text{eff}}^{(2)} \simeq 0$, while in the other extreme of a motor that rests most of the time in rigor will generate a $K_{\text{eff}}^{(2)} \simeq K_{\text{cb}}$ where K_{cb} is the cross-bridge elasticity. The highest frequencies the system can attain at the bifurcation are thus determined by K_{cb} :

$$\omega_{\text{max}} \simeq \left(\frac{\alpha K_{\text{cb}}}{\lambda} - \alpha^2\right)^{1/2}. \quad (17)$$

In the limit of a large number of motors discussed here, the generated oscillations are phase coherent and fluctuations have been neglected. If the number of active elements is finite, the stochasticity of the chemical transitions leads to a stochastic component in the motion. In addition to this noise resulting from active processes, thermal fluctuations can also become relevant. These resulting noisy oscillations have a finite time of phase coherence [17, 15]. While a small number of motors could already generate noisy oscillations with short coherence time, a real Hopf-bifurcation with phase coherent oscillations is only possible as a collective phenomenon of a large number of active elements as described here.

4 Self-organization of motors and filaments

Cilia and flagella which contain an axoneme are important examples of mechanically oscillating biological structures. In these hair-like appendages of many cells, microtubule doublets are arranged in a cylindrical fashion and undergo bending deformations as a result of relative forces exerted by a large number of dynein molecular motors which are densely attached to the surface of microtubules and act on a neighboring microtubules [8], see Fig. 3. At the basal end, microtubules are connected in order to prevent global relative sliding. Internal stresses generated by the motors are thus directly coupled to bending deformations of the elastic microtubule doublets which are all bundled in parallel.

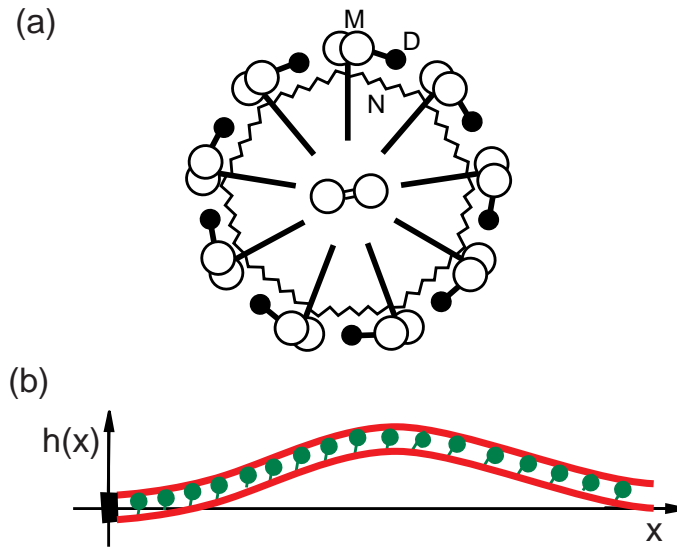


Fig. 3. (a) Schematic representation of the axoneme. Nine microtubule doublets (M) are arranged in a cylindrical fashion around a pair of central microtubules. Dynein motors (D) are attached to the microtubules and exert forces on their neighbors. Elastic elements such as nexins (N) are also present. (b) Two-dimensional representation. Two parallel elastic filaments are connected at one end. Active elements exert internal forces. For small amplitudes, the shape can be characterized by the deformation $h(x)$ as a function of length.

Axonemes are able to generate periodic deformations and to propagate bending waves along the elastic cilium. These systems fall thus in the class of systems where many motors coupled to elastic filaments generate oscillations and spatio-temporal deformation patterns. Basic physical properties of these structures can be captured by considering a two-dimensional version of this system

[24, 44, 45, 25, 26]. Two elastic filaments are arranged in parallel at fixed distance a . At one end both filaments are rigidly connected, everywhere else active elements such as molecular motors induce locally relative sliding of filaments. As motors in this situation generate an increasing displacement, the filament pair bends and generates an elastic force which opposes filament sliding. This situation therefore corresponds to the case discussed in the last section where motors work against an elastic element. Here, this elasticity is provided by the bending elasticity of filaments. If this system undergoes a Hopf bifurcation, the whole filament shape oscillates and exhibits spatio-temporal deformation patterns.

For small deformation amplitudes, the equations of motion of the active filament pair can be discussed in Monge representation, where the perpendicular displacement $h(s)$ as a function of arclength s with $0 < s < L$ is considered. To linear order in h we find,

$$\xi_{\perp} \partial_t h = -\kappa \partial_s^4 h - a \partial_s f \quad (18)$$

where we have assumed for simplicity local viscous friction with coefficient ξ_{\perp} and where $f(t, s)$ is the internal force per unit length exerted by the motors. If the coupled motor-filament system undergoes a Hopf-bifurcation, the selected modes of periodic filament deformations are generic and can be calculated from very few assumptions as long as the system is sufficiently close to the bifurcation such that deformation amplitudes remain small [26].

In this case, we can use Eq. (5) to lowest order to express the relation $f_1(s) \simeq \rho \mathcal{A} \Delta_1(s)$, between the Fourier amplitude of local sliding displacements $\Delta = a(\partial_s h(s) - \partial_s h(0))$ and the amplitude $f_1(s)$ of the density of shear forces, where ρ is the linear density of motors along the filaments. Therefore,

$$i\omega \xi_{\perp} \tilde{h} + \kappa \partial_s^4 \tilde{h} = -a^2 \rho \mathcal{A} \partial_s^2 \tilde{h} \quad (19)$$

together with boundary conditions characterizes the bending patterns selected at a Hopf-bifurcation with critical frequency ω . In this equation, the dynamic linear response function of the motors, \mathcal{A} , plays the role of a complex eigenvalue. At a Hopf bifurcation, \mathcal{A} must take one of a discrete set of complex values. This approach leads to bending waves which propagate along the filament in a direction which depends on the imposed boundary conditions [26]. These patterns only depend on the solvent viscosity and the bending rigidity of microtubules and for given oscillation frequency are independent of the physical details of the mechanism that generates the forces.

The frequency selected by the system however is more difficult to obtain. It depends on properties of the active and passive elements which generate internal shear forces. Two different regimes have to be distinguished: For long filaments complex bending waves are propagated at rather low frequency. For shorter filaments, there exists a simpler regime where filaments vibrate without significant wave propagation. In this latter case, one can ignore to good approximation the detailed shape of the bending patterns. And characterize the deformations simply by a typical deformation amplitude h . We can now think of a situation

where an external force of amplitude F_1 acts on the tip of the vibrating cilium and express the linear response as $h_1 \sim \mathcal{A}_{\text{eff}} F_1$. Approximating the gradient terms in Eq. (19) by their scaling behavior we can write approximately

$$\mathcal{A}_{\text{eff}} \simeq i\omega\xi_{\perp}L + \kappa/L^3 + a^2\rho\mathcal{A}/L \quad (20)$$

Using Eq. (12) to express $\mathcal{A}(\omega, C)$, this leads to

$$\mathcal{A}_{\text{eff}} = k_{\text{eff}} - \gamma_{\text{eff}}\omega^2 + i\omega r_{\text{eff}} \quad (21)$$

where

$$\begin{aligned} k_{\text{eff}} &\simeq \kappa/L^3 + a^2\rho k/L \\ \gamma_{\text{eff}} &\simeq a^2\rho\gamma(\omega)/L \\ r_{\text{eff}} &\simeq a^2\rho r(\omega)/L + \xi_{\perp}L \end{aligned} \quad (22)$$

which allows us to estimate the critical beating frequency of the active filament pair as a function of parameters in several regimes. For example in the case where $\kappa_{\text{eff}} \simeq \kappa/L^3$ and $\xi_{\perp} \gg a^2\rho\lambda/L$ we find

$$\omega_c \simeq \left(\frac{\alpha\kappa}{\xi_{\perp}}\right)^{1/2} \frac{1}{L^2} \quad (23)$$

This result represents a regime in which the system generates oscillations at frequencies which increase significantly for decreasing length if all other parameters are constant. Furthermore, in this simple regime, the frequency is completely determined by the bending rigidity of microtubules κ , the viscosity of the solvent ξ_{\perp} and a typical ATP cycling rate α of the motors.

5 Oscillations in sensory systems: hearing

The cochlea of the inner ear contains about 16000 specialized sensory cells, called hair cells, which are able to detect sounds at a range of frequencies from 50Hz to 40000Hz. The auditory system has an extraordinary dynamic range which covers 120dB or 12 orders of magnitude in sound intensity. Each hair cell has a characteristic frequency at which it is most sensitive. Hair cells are characterized by a bundle of about 50 finger-like structures called stereocilia which have a length of 1-10 μm and a diameter of 300nm. The stereocilia consist predominantly of bundles of actin filaments that are surrounded by a membrane which contains mechano-sensitive ion channels. Upon a tiny shear deformation of the hair bundle of less than a nm, these channels open and the subsequent influx of Potassium and Calcium induced changes in the membrane potential [46] (Fig. 4).

The mechanical response of the basilar membrane, which is the structure inside the cochlea that contains the hair cells, has been measured as a function of frequency and amplitude of sound stimuli [32]. These and other observations

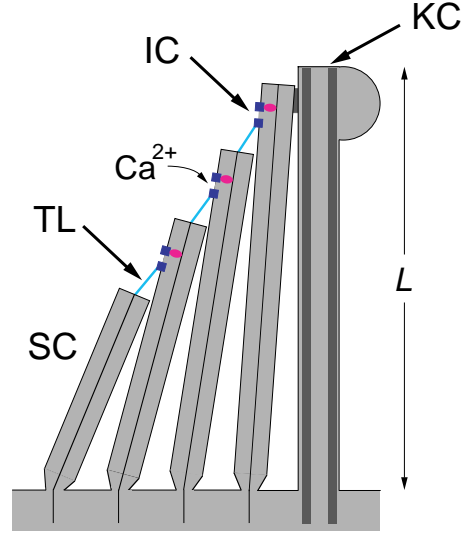


Fig. 4. Schematic representation of the hair bundle of an auditory hair cell. A bundle of stereocilia (SC) containing actin filaments form the hair bundle. They are coupled at their tips by fine filaments called tip-links (TL). The kinocilium (KC) is present in the hair bundles on non-mammalian vertebrates and contains an axoneme. Mechano-sensitive ion channels (IC) open upon a bundle deflection and let to an influx of K^+ and Ca^{++} .

have let to a revival of an idea of Thomas Gold, proposed about 50 years ago [27], that the basilar membrane of the inner ear is not a passively resonating filter as assumed by the classical theory of hearing developed by Van Békésy and others [28]. Instead, Gold suggested that active, energy consuming systems are required by the ear in order to explain some of its extraordinary properties such as a sharp frequency tuning. The mechanical response of the basilar membrane reveals a distinct nonlinear behavior which has all the characteristic properties of a dynamical system placed exactly at a Hopf bifurcation as described in section 2 [15, 16]. Most remarkable is the nonlinear response to stimuli at the critical frequency ω_c , see Eq. (6) which implies a diverging gain $|x_1|/|f_1| \sim |f_1|^{-3/2}$ for small stimulus amplitudes. This nonlinear behavior of the gain and a dramatic increase at small amplitudes has been observed in hearing [32]. This actively enhanced gain together with a power-law nonlinearity provides extraordinary sensitivity and sound detection over a large dynamic range of 6 orders of magnitude in amplitude and 12 orders of magnitude in intensity.

While the properties of a Hopf bifurcation can explain the main properties of sound detection by the ear, it raises a number of important questions. In particular, in order to exhibit a nonlinear response for small amplitudes, the system has to be tuned with high precision to its critical point. This requires a fine-tuning of parameters which raises doubts as to whether a living cell can

profit from the special properties at a critical point in a reliable way.

A simple and general mechanism to maintain a dynamical system at a point of operation close to the bifurcation point can be achieved by a feedback regulation of the control parameter [15, 47]. This self-tuning implies that the control parameter is regulated towards the instability as long as the system is not spontaneously oscillating, while it is automatically stabilized as soon as oscillations are detected. This self-tuning works best in the absence of external stimuli, when highest sensitivity is needed, by adapting the control parameter C as a function of the detected amplitude of hair-bundle deflections.

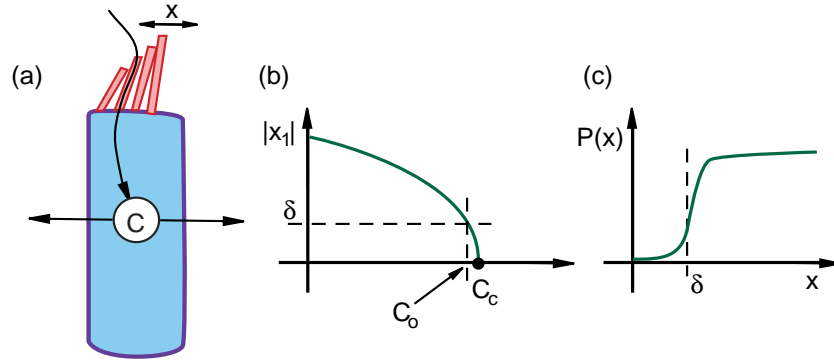


Fig. 5. Simple self-tuning mechanism (schematic). (a) Regulation of the control parameter C associated with the concentration of ions such as Ca^{++} which enter the hair cell via transduction channels. A permanent outflux drives the system towards the oscillating side of the bifurcation, influx of ion via transduction channels provides a stabilizing feedback. (b) Fourier amplitude $|x_1|$ of spontaneous oscillations as a function of the control parameter near the bifurcation point C_c . Self-tuning brings the system to an operating point C_o . (c) Opening probability $P(x)$ of ion channels as a function of the deflection amplitude x . A signal is generated for deflections larger than δ .

An illustrative example for self-tuning is achieved in a situation where the Ca^{++} concentration in the hair cell plays the role of the control parameter at the bifurcation (Fig. 5). Since hair-bundle deflections lead to an influx of Ca^{++} into the hair cell, this provides for a regulation of the control parameter C of the form

$$\frac{dC}{dt} = -\frac{C}{\tau} + JP(x) \quad (24)$$

where τ is a relaxation time of the control parameter in the absence of hair bundle deflections x . This relaxation drives the system in the oscillatory regime. As soon as deflections x occur, ion channels open with probability

$$P(x) = \frac{1}{1 + e^{-(x-\delta)/\ell}} \quad (25)$$

and each open channel gives rise to an influx J of Ca^{++} , which drives the system towards the non-oscillating regime. Here we assume $\tau \gg \omega^{-1}$, i.e. changes in C occur on time-scales long compared to the oscillation frequency. The length scale δ , which for hair bundles is of the order of 0.3-1nm, indicates the smallest deflection amplitudes at which a signal is generated by the hair bundle and the parameter ℓ characterizes the sharpness of the response.

The self-tuning can now be summarized as follows. In the absence of spontaneous oscillations (and if no external sound stimulus is present), the control parameter is decreased within a relaxation time τ . As soon as the critical point C_c is reached, the system starts to oscillate and the decrease of C is halted as soon as the typical oscillation amplitude is of the order of magnitude δ , $|x_1| \sim \delta$. Remember that the onset of spontaneous oscillations in the absence of a force given by Eq. (4) can be expressed as

$$|x_1| \simeq \Delta \left(\frac{C - C_c}{C_c} \right)^{1/2} \quad (26)$$

where Δ is a characteristic saturation amplitude. We can therefore estimate how close to the bifurcation point the system will be tuned via this mechanisms. introducing the distance $\Delta C = C_c - C$ from the bifurcation, the self tuning brings the system slightly to the oscillating side of the bifurcation with

$$\Delta C / C_c \sim (\delta / \Delta)^2 \quad . \quad (27)$$

For a typical hair cell we estimate $\delta \sim 1\text{nm}$ and $\Delta \sim 100\text{nm}$, thus the system can self-tune with $\Delta C / C_c \simeq 10^{-4}$.

These estimates for the useful amplitude range of hair bundle deflections can also explain the dynamic range of hearing. In the regime of nonlinear response, the hair cell can map changes in force amplitude $|f_1|$ that vary by a factor of $(\Delta/\delta)^3 \simeq 10^6$ onto hair bundle deflections $|x_1|$ which vary over the usable range of Δ/δ . This range of detectable force amplitudes corresponds to a dynamic range of 120dB.

The concept of self-tuning to a Hopf bifurcation can explain seemingly disconnected but well-known properties of hearing. In addition to providing an explanation for the high sensitivity at one frequency and a large dynamic range, it can naturally account for what is called adaptation and fatigue. Fatigue implies that the sensitivity to weak stimuli is reduced after a subject is exposed to a loud stimulus which is a natural consequence of self-tuning. In the presence of a stimulus, Eq. (24) tunes the system away from the bifurcation point where sensitivity is reduced. The recovery of high sensitivity after a strong stimulus only happens after a relaxation time τ of the self-tuning feedback to its operation point.

This theory of hearing by a generic mechanism could apply to many different animals such as mammals, birds, reptiles and amphibians. These classes of animals however have different cochleas and different types of hair cells and they might thus use different physical systems to realize a Hopf bifurcation and the

self-tuning. In the case of mammals, there is some evidence that so-called outer-hair cells are able to generate active motion by contracting the whole cell body [29]. Recently, a protein which could play an active role in these contractions has been identified [31]. Non-mammalian vertebrates do not possess outer hair-cells. Active oscillators are therefore expected to exist within the hair bundle itself. Spontaneous hair-bundle oscillations of amphibian hair-cells have been observed and studied in detail [48, 49].

While the physical mechanism at the origin of hair-bundle oscillations remains mysterious, the preceding sections show that molecular motors operating in groups could be responsible for oscillations even at frequencies up to 10kHz. It is well established that myosins occur within the stereocilia and could thus be involved in active movements. Finally, the hair bundles of non-mammalian vertebrates contain in addition to many stereocilia a single cilium which contains an axoneme. Such a structure is ideally suited to play an active role as an oscillator and because of its well-conserved structure, its oscillation frequency could be controlled by just varying its length. If a cilium operates in the regime described by Eq. (23), using a typical $\alpha \simeq 10^3 \text{s}^{-1}$, $\xi_{\perp} = 10^{-3} \text{kg/ms}$ being the viscosity of water and choosing $\kappa = 4 \times 10^{-22} \text{Nm}^2$ which is the bending rigidity of 20 microtubules, the critical frequency is $\omega_c \simeq 2 \times 10^4 \text{s}^{-1}$ for $L = 1 \mu\text{m}$. For $L = 10 \mu\text{m}$, the frequency drops to $\omega_c \simeq 10^2 \text{s}^{-1}$. The physical mechanisms for oscillations generated by molecular motors in a cilium therefore could cover the audible frequency range by using a simple morphological gradient in the cochlea.

6 Discussion

An variety of cells contain structures which are able to spontaneously generate mechanical oscillations. The principal examples discussed here are muscle myofibrils, axonemal cilia and flagella as well as auditory hair cells of the inner ear. While the details of how these oscillations are generated still remain largely unknown, it is expected that motor proteins which undergo a chemical cycle and stochastically generate displacements and forces are the active elements involved. Molecular motors of the cytoskeleton which interact with elastic filaments are omnipresent in eucariotic cells and are likely to be involved in such activities. While in the case of myofibrils and axonemes the crucial role of such motors is established, in the case of hair cells the nature of active proteins is still quite unknown.

The general principles of how oscillations can be generated using such active proteins can be studied using simplified descriptions. Such studies reveal that spontaneous oscillations occur naturally in systems where a large number of active elements and elastic elements interact and form an effective material with active properties. Of particular interest is the Hopf bifurcation where the system becomes unstable with respect to oscillatory behavior. In the vicinity of a bifurcation, the system has generic properties that can be understood and characterized without detailed knowledge of the underlying mechanisms. Furthermore, the bifurcation point has extraordinary response properties which are

ideal to be used for a frequency sensitive detector. A lot of evidence points indeed to the fact that the ear has adopted this principal mechanism, aided by a self-tuning feedback that tunes the oscillators to their critical points.

Phase coherent oscillations and a true Hopf-bifurcation only exist in the thermodynamic limit where an infinite number of active force-generators are present. In a realistic situation with a finite number of molecules present, oscillations are noisy and phase coherence is lost on long times. Oscillations of very few, maybe only a single dynein motors have been reported [50], which however are very noisy. Phase coherent oscillations always result from collective effects in systems with a large number of degrees of freedom. Noise plays an important role for cellular oscillations, in particular in the case of hearing for the detection of weak sounds [15]. A hair cell tuned to its operation point in the absence of an external stimulus will exhibit a spectrum of fluctuations centered around its critical frequency. Because of the active nature of the oscillator, these fluctuations arise partly due to stochastic activity of active elements in addition to thermal noise. As a result of these fluctuations, the hair cell generates already in the absence of any sound hair-bundle motions which have a strong fluctuating component. Consequently, unstimulated hair-cells already generate action potentials at low rate. Because of their stochastic nature these action potentials can be distinguished from the excitation due to a sinusoidal stimulus. As soon as a weak stimulus is present, its main effect is to phase lock the spontaneous motion. This phase locking to a stimulus can be detected before amplitude changes occur. By this mechanism the ear can detect sounds which have an effect on the amplitude that is smaller than the noise.

Oscillatory behaviors are also observed in very different types of systems. An interesting example are lymphoblasts which usually do not show oscillatory behaviors. However, if the microtubule network is depolymerized using nocodazole, the cell attains a state where the actin system forms a contractile ring which generates a constriction of the cell. Interestingly, this ring slowly oscillates between the two poles of the cell [51]. The mechanism leading to these oscillations is not understood. However, it is likely that these oscillations are a result of a self-organization of the actin cytoskeleton with the help of myosin motors and maybe other components.

The self-organization of motors and filaments can lead to complex phenomena in various situations. Such phenomena have in particular been studied in filament systems which are driven by molecular motors that temporarily form active crosslinks between filament pairs. In such active filament systems, complex behaviors such as contractions and the formation of asters and spirals have been observed [52, 53, 54, 55, 56]. A phenomenological description of the dynamics of active filament bundles can be used to describe tension generation and contractions in non-organized bundles [57]. This description takes into account two different filament interactions: (i) interactions between parallel filaments which point in the same direction and (ii) between filaments that are anti-parallel. If both interactions are present at the same time, the system can generate patterns of contracted regions along the bundle which propagate. In periodic systems such

as contractile rings, this can lead to oscillatory behaviors of bundle contractions [58].

Mechanical oscillations in cells thus occur in a large variety of different situations and with frequencies which can vary over large ranges. Slow oscillations of contractile rings start from several minutes per period; the highest frequencies of active oscillations in hair cells could exceed 100kHz, e.g. during high frequency sound detection in bats and whales.

I thank S. Camalet, T. Duke, K. Kruse and J. Prost for stimulating collaborations and A. Ajdari, M. Bornens, H. Delacroix, R. Everaers, A.J. Hudspeth, A. Maggs, P. Martin for helpful discussions.

References

1. Kreis T., and Vale R. (1993): *Cytoskeletal and Motor Proteins*, (Oxford University Press, New York).
2. Alberts B., Bray D., Lewis J., Raff M., Roberts K. and Watson J.D. (1994): *The molecular biology of the cell*, (Garland, New York).
3. Pringle J.W.S. (1977): in *Insect Flight Muscle*, R.T. Tregear, Ed. , North-Holland, Amsterdam, 177.
4. Yasuda K., Shindo Y. and Ishiwata S. (1996): *Biophys. J.* **70**, 1823.
5. Fujita H. and Ishiwata S. (1998): *Biophys. J.* **75**, 1439.
6. Bray D. (1992), *Cell Movements* (New York, Garland).
7. Murase M. (1992): *The dynamics of cell motility* (New York, Wiley).
8. Lindemann C.B. and Kanous K.S. (1997): *Int. Rev. Cytology* **173**, 1.
9. Gibbons I.R. (1975): in *Molecules and Cell Movement*, S. Inoué and R.E. Stephens (Eds.), Raven Press, New York.
10. Brokaw C.J. (1991): *J. Cell. Biol.* **114**, 1201.
11. Brokaw C.J. (1996): *Cell. Mot. Cytoskel.* **33**, 6.
12. Taylor G.I. (1951): *Proc. R. Soc. A* **209**, 447.
13. Purcell E.M. (1977): *Am. J. Phys.* **45**, 3.
14. Strogatz S.H. (1994): *Nonlinear Dynamics and Chaos* (Addison-Wesley, Reading, MA).
15. Camalet S., Duke T., Jülicher F. and Prost J. (2000): *Proc. Natl. Acad. Sci.* **97**, 3138.
16. Eguiluz V.M., Ospeck M., Choe Y., Hudspeth A. J. and Magnasco M.O. (2000): *Phys. Rev. Lett.* **84**, 5232.
17. Jülicher F., and Prost J. (1997): *Phys. Rev. Lett.* **78**, 4510.
18. Jülicher F., Ajdari, A. and Prost J. (1997): *Rev. Mod. Phys.* **69** 1269.
19. Huxley A.F. (1957): *Prog. Biophys.* **7**, 255.
20. Jülicher F., and Prost J. (1995): *Phys. Rev. Lett.* **75**, 2618.
21. Riveline D., Ott A., Jülicher F., Winkelmann D.A., Cardoso O., Lacapère J.-J., Magnusdottir S., Viovy J.-L., Gorre-Talini L. and Prost J. (1998): *Eur. Biophys. J.* **27** 403.
22. Reimann P., Kawai R., Van den Broek C., and Hänggi P. (1999): *Europhys. Lett.* **45**, 545.
23. Reimann P. (2000): preprint cond-mat/0010237.
24. Brokaw C.J. (1975): *Proc. Natl. Acad. Sci.* **72**, 3102.

25. Camalet S., Jülicher F., and Prost J. (1999): Phys. Rev. Lett. **82**, 1590.
26. Camalet S. and Jülicher F. (2000): New. J. Phys. **2** (2000) 24, 1.
27. Gold T. (1948): Proc. R. Soc. B **135**, 492.
28. von Békésy, Experiments in Hearing (McGraw Hill, New York).
29. Dallos P.J. (1992): J. Neurosci. **12**, 4575.
30. Hudspeth A.J. (1997): Curr. Opin. Neurobiol. **7**, 480.
31. Zheng J. et al. (2000): Nature **405**, 155.
32. Ruggero M.A. (1992): Curr. Opin. Neurobiol. **2**, 449.
33. Bialek W. (1987): Annu. Rev. Biophys. Chem. **16**, 455.
34. Jülicher F., Andor D. and Duke T., in preparation.
35. Van der Pol B. (1926): Phil. Mag. **2**, 978.
36. Nayfeh A.H., Mook D.T. (1979): Nonlinear oscillations, Pure and applied mathematics (Wiley, New York).
37. Ajdari A., and Prost J. (1992): C.R. Acad. Sci. Paris II, **315**, 1635.
38. Magnasco M.O. (1993): Phys. Rev. Lett. **71** 1477 (1993).
39. Prost J., Chauwin J.F., Peliti L., and Ajdari A. (1994): Phys. Rev. Lett. **72**, 2652.
40. Astumian R.D., and Bier M. (1994): Phys. Rev. Lett. **72**, 1766.
41. Peskin C.S., Ermentrout G.B., and Oster G.F. (1994): *Cell Mechanics and Cellular Engineering*, V.Mow et al eds. (Springer, New-York).
42. Astumian R.D. (1997): Science **276**, 917.
43. F. Jülicher (1999): in Transport and Structure: Their Competitive Roles in Biophysics and Chemistry edited by S.C. Miller, J. Parisi and W. Zimmermann, Lecture Notes in Physics, Springer (Berlin).
44. Hines M. and Blum J.J. (1978): Biophys. J. **23**, 41.
45. Brokaw C. (1985): Biophys. J. **48**, 633.
46. Hudspeth A.J. and Gillespie P.G. (1994): Neuron **12**, 1.
47. Camalet S. (2001): Thèse Université Paris 6.
48. Martin P. and Hudspeth A.J. (1999): Proc. Natl. Acad. Sci. USA **96**, 14306.
49. Martin P., Metha A.D. and Hudspeth A.J. (2000): Proc. Natl. Acad. Sci. **97**, 12026.
50. Shingyoji C., Higuchi H., Yoshimura M., Katayama E. and Yanagida T. (1998): Nature **393**, 711.
51. Bornens M., Paintrand M. and Celati C. (1989): J. Cell. Biol. **109**, 1071 (1989).
52. Takiguchi K. (1991): J. Biochem. **109**, 502.
53. Nédélec F.J. et al. (1997): Nature (London) **389**, 305.
54. Surrey T. et al. (1998): Proc. Natl. Acad. Sci. USA **95**, 4293.
55. Nakazawa H. and Sekimoto K. (1996): J. Phys. Soc. Japan **65**, 2404.
56. Sekimoto K. and Nakazawa H. (1998): in *Current Topics in Physics*, Y.M. Cho, J.B. Hong, and C.N. Yang (eds.) vol1, p.394 (World Scientific, 1998); physics/0004044.
57. Kruse K. and Jülicher F. (2000): Phys. Rev. Lett. **85**, 1778.
58. Kruse K., Camalet S. and Jülicher F., unpublished.